Journal of Thermal Analysis and Calorimetry, Vol. 72 (2003) 105–111

THERMAL EVOLUTION OF FERROMAGNETIC METALLIC GLASSES
A study using TG(M) technique

G. Luciani [1, 2*], *A. Costantini* [1], *F. Branda* [1], *P. Scardi* [3] *and L. Lanotte*[2]

[1]Dipartimento di Ingegneria dei Materiali e della Produzione, Università di Napoli 'Federico II', p. le Tecchio 80, 80125 Napoli, Italy
[2]Istituto Nazionale per la Fisica della Materia – INFM, Università di Napoli 'Federico II', p. le Tecchio 80, 80125 Napoly, Italy
[3]Dipartimento di Ingegneria dei Materiali, Università di Trento, Via Mesiano 77, 38050 Trento, Italy

Abstract

A traditional TG apparatus was modified by placing two permanent magnets producing a controlled magnetic field (TG(M): Magneto Thermogravimetry). This technique proved to be useful to study both structural relaxation and crystallisation of ferromagnetic metallic glasses. Results obtained for the amorphous alloys $Fe_{40}Ni_{40}P_{14}B_6$ and $Fe_{62.5}Co_6Ni_{7.5}Zr_6Nb_2Cu_1B_{15}$, are reported in this paper.

Structural relaxation can be evaluated by measuring changes in Curie temperature induced by thermal treatments.

Crystallisation in TG(M) is detected through a change in the measured apparent mass (difference between the sample mass and magnetic force driving it upward). These results were confirmed by DSC analysis.

Whether the obtained crystalline phase is ferromagnetic, it can be identified through its Curie temperature, measured by TG(M). In fact the value of 770°C measured as Curie temperature of crystallised $Fe_{62.5}Co_6Ni_{7.5}Zr_6Nb_2Cu_1B_{15}$,led to conclude that the only ferromagnetic crystalline phase is α-Fe. These hypothesis was confirmed by XRD analysis, showing that the first crystallisation yields to α-Fe nanocrystals.

Keywords: amorphous alloys, crystallization, Curie temperature, DTA, TG(M)

Introduction

Melt-spun ribbons of metastable, soft ferromagnetic alloys have been competing with the older crystalline soft magnetic materials since 1970s. Recently they gained renewed interest as core of magneto-elastic sensors for vibration and displacement detection without contact [1]. In fact, high magnetoelastic waves amplitude can be obtained for their high magnetoelastic coupling factor, Young's modulus and magnetic permeability at low field [2, 3]. Moreover, in these applications, the magnetoelastic response is generally enhanced in materials where a nearly complete structural relaxation and a partial nanocrystallisation are induced by thermal treatment [4–6].

* Author for correspondence: E-mail: luciani@cds.unina.it

1388–6150/2003/ $ 20.00

Akadémiai Kiadó, Budapest
Kluwer Academic Publishers, Dordrecht

On the basis of these observations, a ferromagnetic alloy of nominal composition $Fe_{62.5}Co_6Ni_{7.5}Zr_6Cu_1Nb_2B_{15}$, has recently been proposed for use in magnetoelastic devices [7]. The alloy components were calibrated to have a very soft magnetic material, showing giant amplitude of resonant magnetoelastic waves at zero magnetising field [8].

Since structural, mechanical and magnetic properties are strictly related, studying thermal induced phase transitions in the amorphous structure, their kinetic and their influence on magnetic properties is fundamental to pick out which thermal treatment can induce the best soft ferromagnetic and magnetoelastic properties. Crystallisation of amorphous alloys was studied in previous works using TG(M) and DTA [9–13]. Furthermore, structural relaxation phenomena occurring during isothermal annealing and their influence on magnetic properties were investigated [7, 8, 14–16]. This paper shows potentialities of Magneto Thermogravimetric Analysis (TG(M)) to investigate both crystallisation and structural relaxation of metallic glasses.

Experimental

The amorphous alloys were prepared by one-roll melt-spinning technique, with a quenching rate of 28 m s^{-1}, starting from a precursor alloy produced by arc melting in a quartz crucible in Ar atmosphere. Ribbons of $Fe_{62.5}Co_6Ni_{7.5}Zr_6Cu_1Nb_2B_{15}$ and $Fe_{40}Ni_{40}P_{14}B_6$ were 30 μm×3 mm×several metres. The composition of the specimens was checked by Wavelength Dispersive X-ray spectrometry (WDX).

Differential scanning calorimetric (DSC) analysis was carried out by means of a Netzsch heat flux DSC apparatus, model 404 M, on cut ribbons at a heating rate β=20°C min^{-1}.

Thermogravimetric analysis (TG) was carried out by means of a Netzsch thermo-microbalance apparatus (model TG209) on short (1 cm long) ribbons of about 2 mg in mass. Isothermal treatments were performed in argon atmosphere. The samples, before and after isothermal treatment, were heated in the TG(M) apparatus at a heating rate of β=20°C min^{-1} in argon atmosphere and the change in apparent mass due to the applied magnetic field was measured. It is known [17] that temperature for a TG apparatus can be calibrated by means of the Curie temperatures (T_c) of known ferromagnetic materials. At T_c ferromagnetic materials turns into paramagnetic and a sudden apparent mass increase is recorded.

X-Ray Diffraction (XRD) patterns were collected on PMG-VH Rigaku diffractometer using the conventional Bragg-Brentano geometry. The system was equipped with a diffracted beam graphite crystal analyser and suitably narrow slits (Soller, incident, divergence and antiscattering) so as to produce a nearly zero background and narrow and symmetrical instrumental profiles, even for 2θ angles as low as 20–25° [18]. The Instrumental Resolution Function (IRF), describing the change in profile width and shape with the 2θ angle was determined using a suitable KCl powder sample, and analytically described by means a non-linear least square fitting of pseudo-Voigt function for the $CuK\alpha_1$, α_2 doublet [19].

Results

Figure 1 shows a typical TG(M) curve recorded on a ferromagnetic amorphous alloy. A steep increase in mass is measured on heating due to the transition from ferromagnetic to paramagnetic behaviour at Curie temperature, T_c. At lower temperatures than T_c when a magnetic field is applied an apparent mass is measured, that is the difference between the sample mass and the vertical component of magnetic force. At temperatures above the Curie point, the real mass of the sample is recorded. Figure 2 shows Curie temperatures as a function of temperature of isothermal treatment for $Fe_{40}Ni_{40}P_{14}B_6$ and $Fe_{62.5}Co_6Ni_{7.5}Zr_6Nb_2Cu_1B_{15}$. A minimum in Curie temperature is recorded for $Fe_{62.5}Co_6Ni_{7.5}Zr_6Nb_2Cu_1B_{15}$ after isothermal annealing for 1 h at T=380°C; while a more complicated trend is observed for the former.

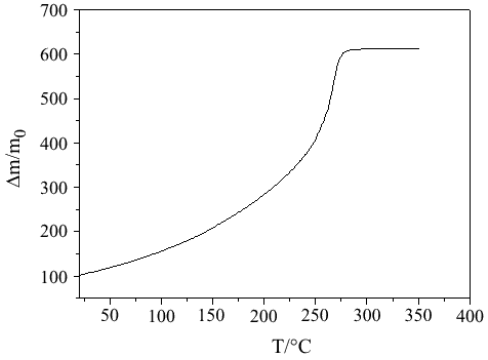

Fig. 1 A typical TG(M) curve of a ferromagnetic alloy

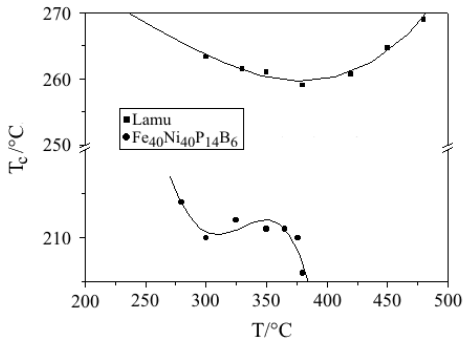

Fig. 2 T_c temperatures *vs*. temperature of isothermal annealing

Figure 3 shows TG and DTA curves recorded, at a heating rate β=20°C min^{-1}, on an as-cast $Fe_{62.5}Co_6Ni_{7.5}Zr_6Nb_2Cu_1B_{15}$ samples. The DTA curve shows a complex crystallisation process, in several steps, each corresponding to an exothermic peak. A decrease in apparent mass on TG(M) curve starts from 539°C, corresponding to the first crystallisation onset on the DTA curve. A good correspondence can be also observed between the 3rd and 4th crystallisation peak and apparent mass changes recorded at higher temperatures in TG(M). Figure 4a shows TG(M) and DTA curves

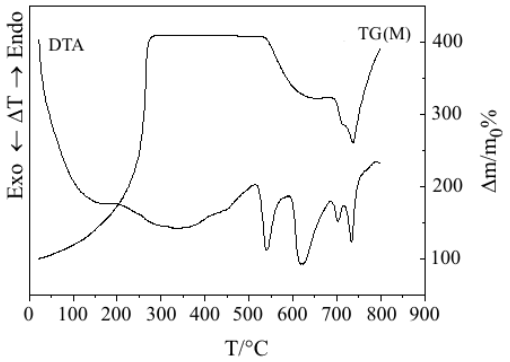

Fig. 3 DTA and TG(M) curves recorded on $Fe_{62.5}Co_6Ni_{7.5}Zr_6Nb_2Cu_1B_{15}$

obtained on $Fe_{40}Ni_{40}P_{14}B_6$. No effect was recorded on the TG(M) curve at crystallisation. However the TG(M) curve recorded on cooling showed (Fig. 4b) a different trend from what observed on heating (Fig. 4a). TG curves recorded without external magnetising field are shown in Fig. 5, proving that oxidation causes smaller changes in mass, only 5%, than changes in apparent mass measured in presence of magnetic field. Moreover, $Fe_{62.5}Co_6Ni_{7.5}Zr_6Nb_2Cu_1B_{15}$ is more resistant to oxidation than $Fe_{40}Ni_{40}P_{14}B_6$.

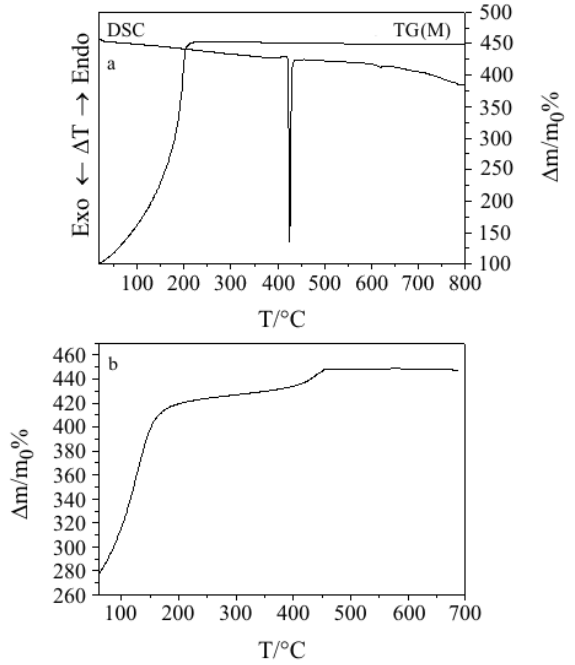

Fig. 4 a – DTA and TG(M) curves recorded for $Fe_{40}Ni_{40}P_{14}B_6$ on heating; b – TG(M) curve recorded for $Fe_{40}Ni_{40}P_{14}B_6$ on cooling

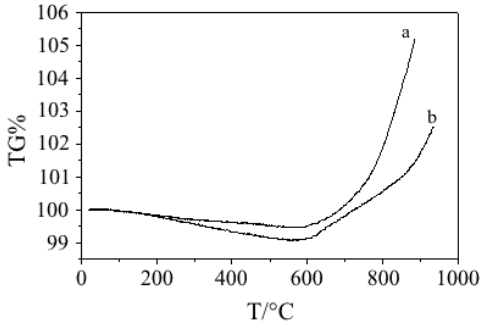

Fig. 5 TG curves recorded at 20°C min^{-1} a – $Fe_{40}Ni_{40}P_{14}B_6$; b – $Fe_{62.5}Co_6Ni_{7.5}Zr_6Nb_2Cu_1B_{15}$

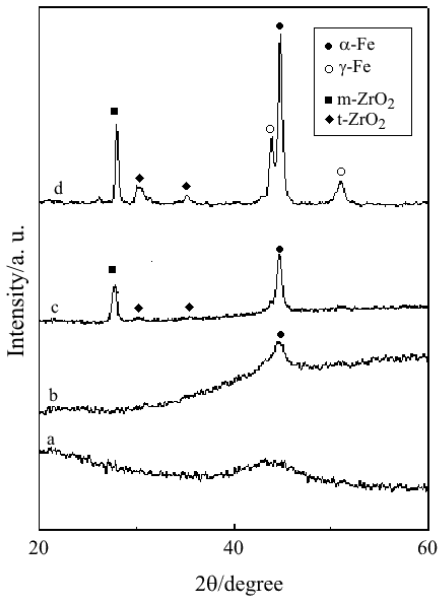

Fig. 6 XRD patterns of $Fe_{62.5}Co_6Ni_{7.5}Zr_6Nb_2Cu_1B_{15}$ samples a – as-quenched; b–d – submitted to DTA cycle stopped at b – I exo-peak; c – II exo-peak; d – after the last exo-peak

The XRD patterns of variously heat treated samples are reported in Fig. 6. The as-cast sample (Fig. 6a) confirmed to be amorphous. Figures 6b, c and d refer to samples submitted, in the DSC apparatus, to non-isothermal heat treatments at a heating rate β=20°C min^{-1} stopped at the first and second peak, and after the last exo-peak, respectively. Pattern 6b shows a broad XRD reflection corresponding to the strongest line of α-Fe. In Fig. 6c (2^{nd} exo-peak) this reflection becomes sharper and a second one appears at $2\theta \cong 28°$ with other minor peaks at ~30.2 and ~35.2°. In the XRD pattern of the sample heated up to 750°C (Fig. 6d) the reflections of γ-Fe also appear clearly.

Discussion

Rapid quenching of metallic melts gives amorphous alloys with a more or less large excess-volume; when heat-treated in the glass transformation temperature range they undergo crystallisation. However, important structural changes occur at lower temperatures where long range diffusion is hindered. At these temperatures topological (TSRO) or chemical (CSRO) short-range ordering occur [20, 21]. They affect both the Curie temperature and the induced magnetic anisotropy [22]. Therefore T_c changes recorded after an isothermal treatment (Fig. 2), can be ascribed to structural relaxation induced by the thermal treatment. The minimum recorded for T_c of $Fe_{40}Ni_{40}P_{14}B_6$ can be explained by admitting two relaxation mechanisms having very different relaxation times [23], with a cross-over temperature T=300°C as found in a previous work [12].

The increase of T_c temperature observed for Lamu at higher temperature than 380°C (Fig. 2) can be explained assuming a longer range atomic reorganization, in the glass transition range, before crystallisation, as confirmed by Extended X-Ray Absorption Fine Structure (EXAFS) results [24].

The recorded decrease in apparent mass (Fig. 3) starting from 539°C, in the crystallisation temperature range, is due to the growth of a ferromagnetic crystalline phase. Further decreases in apparent mass are observed on the TG(M) curve in the temperature range of the 3rd and 4th DSC crystallisation peaks. The steep change shown on TG(M) curve of $Fe_{62.5}Co_6Ni_{7.5}Zr_6Nb_2Cu_1B_{15}$ at 770°C is due to ferromagnetic-paramagnetic transition of at least one of the formed crystalline phases. That value corresponds to Curie temperature of α-Fe. This is confirmed by XRD results (Fig. 6). In fact, the XRD patterns of Fig. 6 clearly show that the first exo-peak corresponds to the crystallisation of α-Fe (Fig. 6b). The second crystallisation peak mainly corresponds to the growth of γ-Fe paramagnetic crystals (Fig. 6c) as supported by the much lower apparent mass change recorded in TG(M) (Fig. 3). The 3rd and the 4th exothermic DTA peaks (Fig. 3) can be attributed to a re-crystallisation of α-Fe and γ-Fe (Fig. 6c). The reflection at $2\theta \cong 28°$ is attributed to an oxidation product. Its appearance starting from the 6c pattern is consistent with the TG curve recorded in absence of magnetic field (Fig. 6) showing mass increase starting from 580°C, which approximately corresponds to the onset of the second DTA exo-peak. It was attributed to the strongest line (111) of monoclinic ZrO_2 (*m*-ZrO_2); the absence of the other lines of *m*-ZrO_2 would imply an epitaxial growth of the oxide film. Reflections at $2\theta \cong 30.2$ and 35.2° can indeed be attributed to tetragonal ZrO_2 (*t*-ZrO_2).

No effect was recorded on the TG(M) curve of $Fe_{40}Ni_{40}P_{14}B_6$ at crystallisation (Fig. 4), therefore the formed crystalline phase must be paramagnetic in that temperature range. This is confirmed by the TG(M) curve recorded on cooling, showing three T_c values, all lower than DTA exothermic peak temperature, T_p.

Conclusions

In the studied metallic glasses, topological and chemical short range ordering are induced by annealing below first crystallisation temperature. These structural evolu-

tions have magnetic and elastic properties changed. Therefore, a comprehension of these mechanisms is required to choose the thermal treatment producing a proper response for application purposes. TG(M) apparatus is a powerful technique to study both structural relaxation and crystallisation of ferromagnetic metallic glasses. Moreover, for $Fe_{62.5}Co_6Ni_{7.5}Zr_6Nb_2Cu_1B_{15}$ metallic glass, it led to the identification of the formed crystalline phase.

References

1 M. Vazquez and H. Hernando, J. Phys. D, 29 (1996) 271.
2 E. Olsen, Applied Magnetism, Philips Technical Library, Eindhoven (The Netherlands) 1966.
3 V. Iannotti and L. Lanotte, Phil. Mag. B, 80 (2000) 1903.
4 Les Amorphes Metalliques, Les Editions de Physique Editor, Proceeding of Ecole d'Hiver-Aussois, 1983.
5 R. Hasegawa, J. Magn. Mater., 100 (1991) 1.
6 Z. Kaczkowski, L. Malinski and M. Muller, IEEE Trans. Magn., 31 (1995) 155.
7 L. Lanotte, V. Iannotti and M. Muller, J. Appl. Electromagn. Mech., 10 (1999) 215.
8 L. Lanotte, G. Ausanio, M. Carbucicchio, V. Iannotti and M. Muller, J. Magn. and Magn. Mat., 215–216 (2000) 276.
9 J. J. Suñol, N. Clavaguera and M. T. Mora, J. Therm. Anal. Cal., 52 (1998) 853.
10 D. M. Lin, H. S. Wang, M. L. Lin and Y. C. Wu, J. Therm. Anal. Cal., 58 (1999) 347.
11 D. M. Lin, M. L. Lin, M. H. Lin, Y. C. Wu, H. S. Wang and Y. J. Chen, J. Therm. Anal. Cal., 58 (1999) 355.
12 F. Branda, G. Luciani and A. Costantini, J. Therm. Anal. Cal., 61 (2000) 889.
13 J. J. Suñol, M. T. Clavaguera-Mora and N. Clavaguera, J. Therm. Anal. Cal., 70 (2002) 173.
14 G. Ausanio, V. Iannotti, C. Luponio and L. Lanotte, Mat. Sci. Tech., 17 (2001) 1525.
15 P. Allia, M. Coisson, P. Tiberto, F. Vinai and L. Lanotte, J. Magn. Magn. Mater., 215–216 (2000) 346.
16 L. Lanotte, G. Ausanio, V. Iannotti, F. Branda, G. Luciani, A. Stantero, F. Vinai and M. Carbucicchio, Nanostructure Materials, 11 (1999) 805.
17 M. E. Brown, Thermal Analysis – Techniques and Applications, Chapman and Hall, London 1988.
18 P. Scardi, L. Lutteroti and P. Maistrelli, Powder Diffraction, 9 (1994) 180.
19 M. Leoni, P. Scardi and J. I. Langford, ibid. 13 (1998) 210.
20 P. H.Gaskell, J. Non-Cryst. Solids, 32 (1979) 207.
21 H. Herman and W. Kreher, J. Phys. F: Met. Phys., 18 (1988) 641.
22 C. D. Graham Jr. and T. Egami, J. Magn. Magn. Mat., 15–18 (1980) 1325.
23 A. L. Greer and J. A. Leak, J. Non-Cryst. Solids, 33 (1979) 291.
24 G. Ausanio, V. Iannotti, F. Miletto Granozio, C. Meneghini, M. Minicucci, F. Ricci and L. Lanotte, J. Magn. Magn. Mat., 242–245 (2002) 904.